First-principles study of the electronic structure and optical properties of cubic Perovskite $NaMgF_3$*

Li Zhen-Li(李贞丽)[a)b)], An Xin-You(安辛友)[b)], Cheng Xin-Lu(程新路)[a)], Wang Xue-Min(王雪敏)[b)], Zhang Hong(张 红)[a)], Peng Li-Ping(彭丽萍)[b)†], and Wu Wei-Dong(吴卫东)[b)]

[a)] *Institute of Atomic and Molecular Physics, Sichuan University, Chengdu* 610064, *China*

[b)] *Science and Technology on Plasma Physics Laboratory, Research Center of Laser Fusion, Chinese Academy of Engineering Physics, Mianyang* 621900, *China*

(Received 31 July 2013; revised manuscript received 17 September 2013; published online 24 January 2014)

The structural, electronic, and optical properties of cubic perovskite $NaMgF_3$ are calculated by plane-wave pseudopotential density functional theory. The calculated lattice constant a_0, bulk modulus B_0, and the derivative of bulk modulus B_0' are 3.872 Å, 78.2 GPa, and 3.97, respectively. The results are in good agreement with the available experimental and theoretical values. The electronic structure shows that cubic $NaMgF_3$ is an indirect insulator with a wide forbidden band gap of $E_g = 5.90$ eV. The contribution of the different bands is analyzed by total and partial density of states curves. Population analysis of $NaMgF_3$ indicates that there is strong ionic bonding in the MgF_2 unit, and a mixture of ionic and weak covalent bonding in the NaF unit. Calculations of dielectric function, absorption coefficient, refractive index, electronic energy loss spectroscopy, optical reflectivity, and conductivity are also performed in the energy range 0 to 70 eV.

Keywords: density functional theory, cubic perovskite $NaMgF_3$, electronic properties, optical properties

PACS: 71.15.Mb, 71.20.–b, 78.20.Ci **DOI:** 10.1088/1674-1056/23/3/037104

1. Introduction

Perovskite-type fluorides have gained significant attention due to their great potential applications in optical, ferroelectric, and antiferromagnetic systems.[1–4] As important inorganic functional materials, ternary cubic fluoroperovskites of type ABF_3 (A = Li, Na, K, Rb, Cs; B = divalent-metal) with interesting optical and magnetic properties have been applied as luminescent materials, radiation detectors, and laser optical materials.[5] For example, Cs-based $CsMF_3$ (M = Be, Mg, Ca, Sr, Cd, and Hg) shows potential in the field of luminescence.[6] $BaLiF_3$ can be used as vacuum-ultraviolet-transparent material for lenses in optical lithography steppers.[7] $CsCaF_3$ and $KMgF_3$ have many applications in tunable lasers due to their unique properties,[8,9] and furthermore, $KMgF_3$ can be used in electro-optical applications.[10,11] In this family, the $NaMgF_3$ crystal exhibits a wide variety of physical properties.[12] Natural $NaMgF_3$ was first discovered in the 1960s,[13] but systematic studies of $NaMgF_3$ did not begin until two decades ago. Intensive studies of the structure of $NaMgF_3$ for its temperature-induced phase transition at ambient pressure and under high-pressure conditions were carried out by Zhao *et al.*[14–17] They found that $NaMgF_3$ is a stable *Pbnm* perovskite phase at ambient conditions and undergoes a transition to a cubic phase when elevating the temperature up to 765 °C. Chen *et al.*[18] reported that the same structural phase transition takes place at 4 GPa when the temperature is increased from 900 °C to 1000 °C. In addition, Zhao *et al.* also synthesized the single crystal of neighborite using the melting-cooling method, and measured its adiabatic elastic moduli at ambient conditions using Brillouin spectroscopy.[19] Andersen *et al.*[20] carried out a study of the ionic conductivity of $NaMgF_3$ and found no abnormal ionic conductivity at high temperatures. Seretlo *et al.*[21] studied the optical absorption of radiation-produced defects in $NaMgF_3$ and $RbCaF_3$. Subsequently, the near-normal incidence reflection spectra of $NaMgF_3$ and $KMgF_3$ have been measured in the extreme ultraviolet region using synchrotron radiation, and the dielectric constant was obtained by means of the Kramers–Kronig transformation.[12] Sevonkaev *et al.* prepared uniform cubic particles of neighborite ($NaMgF_3$) by mixing solutions of magnesium chloride and sodium fluoride, followed by aging for extended periods of time (up to 3 h). However, they did not give further analysis of the neighborite crystallites.[22] Following which, Zhang *et al.* synthesized the fluoroperovskite $NaMgF_3$ by the solvothermal method, and then demonstrated a strong emission center at 400 nm at room temperature.[23] More recently, Li *et al.* carried out mechanical oscillation experiments of polycrystalline $NaMgF_3$ perovskite at high pressures and temperatures.[24]

Though a substantial amount of experimental information has been accumulated on $NaMgF_3$, the theoretical properties have rarely been addressed. In this paper, we focus on the theoretical study of the cubic perovskite $NaMgF_3$, in which the MgF_6 unit is a perfect octahedron and tilt is forbidden, and all the Mg–F angles are 90°. We calculated the electronic and optical properties of cubic $NaMgF_3$ by performing density func-

*Project supported by the National Natural Science Foundation of China (Grant No. 11176020).

†Corresponding author. E-mail: pengliping2005@126.com

© 2014 Chinese Physical Society and IOP Publishing Ltd

tional theory (DFT) with local density approximations (LDA) to obtain a further understanding of this compound. Since there have been fewer theoretical reports on $NaMgF_3$, the results obtained in our work may be useful for other groups and may provide an important reference for the application of $NaMgF_3$ in practice. This paper is organized as follows: the computational method is described in Section 2, the obtained results are presented and discussed in Section 3, and the conclusion is given in Section 4.

2. Computational method

The calculations were performed within the framework of DFT[25] using the plane-wave pseudopotential scheme[26] with the Ceperley–Alder form of the LDA.[27,28] The Na 3s1, Mg 3s2, F 2s2, 2p5 electrons were explicitly treated as valence electrons. The plane-wave basis set with an energy cutoff of 500 eV was applied, and Brillouin zone integration was performed over $10\times10\times10$ grid points using the Monkorst–Pack method[29] for structure optimization. The self-consistent convergence of the total energy was about 2.0×10^{-5} eV per atom. The maximum atom force was less than 0.05 eV/Å, the maximum atom displacement was less than 0.002 Å, and the maximum stress was within 0.1 GPa. All the total energy calculations were performed using the Cambridge serial total energy package (CASTEP) code.[30,31]

3. Results and discussion

3.1. The structure of cubic perovskite $NaMgF_3$

The crystal structure of cubic perovskite $NaMgF_3$ belongs to the space group $Pm3m$ with Na at (0, 0, 0), Mg at (0.5, 0.5, 0.5), and F at (0.5, 0.5, 0) positions, as shown in Fig. 1(a). The calculated total energy per unit cell of cubic $NaMgF_3$ as a function of volume is displayed in Fig. 1(b). The volume versus energy was fitted to the Birch–Murnaghan equation of state[32] so as to determine the equilibrium structural parameters. Then, the equilibrium lattice constant a_0, equilibrium energy E_0 per unit cell at volume V_0, bulk modulus B_0, and pressure derivative of the bulk modulus B_0' were obtained. These values are listed in Table 1. It is clear that the calculated equilibrium lattice constant $a_0 = 3.872$ Å is in excellent agreement with the experimental values. Additionally, we calculated the lattice parameters of orthorhombic ($pbnm$) $NaMgF_3$ for the sake of comparison with the experimental data. Our calculated lattice parameters are $a = 5.262$ Å, $b = 5.455$ Å, $c = 7.559$ Å, which agree reasonably well with the experimental results (at 4 GPa at a temperature of 25 °C[18] and at ambient pressure at 332 K[33]), indicating the rationality of our selected pseudopotential and exchange-correlation function.

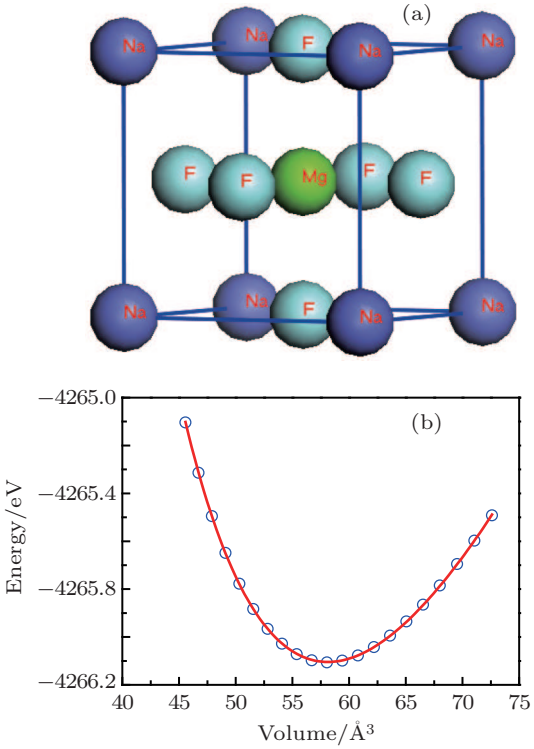


Fig. 1. (color online) (a) The structure of cubic perovskite $NaMgF_3$, and (b) the volume versus energy of cubic perovskite $NaMgF_3$.

Table 1. The calculated lattice constants a_0, bulk modulus B_0, pressure derivative of bulk modulus B_0', and equilibrium volume V_0 of cubic $NaMgF_3$.

a_0/Å	B_0/GPa	B_0'	V_0/Å^3
3.872(3.955[a], 3.833[b], 3.876[c], 3.836[d], 3.840[e])	78.2 (87.999[d])	3.97	58.05

[a] [b] [c](Experiment),[13,14,18] [d]*ab initio* perturbed ion calculations,[34] [e]*a priori* calculation.[35]

3.2. The band structure and density of states

The computed electronic energy band structure along the high-symmetry directions in the first Brillouin zone of $NaMgF_3$ is shown in Fig. 2. Table 2 presents the band-gap energies along with the valence-to-conduction band transition for cubic $NaMgF_3$. $NaMgF_3$ has a conduction band minimum (CBM) at the Γ point and valence band maximum (VBM) at the R point. The band-gap width E_g is 5.90 eV ($R \to \Gamma$). Thus, $NaMgF_3$ is an indirect and wide band-gap insulator. To further elucidate the nature of the electronic band structure, we also calculated the total and partial density of states (TDOS and PDOS) of $NaMgF_3$, as shown in Fig. 3. In the valence band, the band with the lowest energy, between −48.38 eV and −46.53 eV, is dominated by the Na 3s states. The band from

−37.42 eV to −35.53 eV is a contribution mainly from Mg 2p states. The bands lying between −21.03 eV and −18.23 eV are hybridized with the F 2s and Na 2p states, and form two separate peaks in the total density of states. The bands from −5.12 eV to the Fermi level (at 0 eV) originate from the F 2p states. In the conduction band, the bands starting from 5.12 eV to 25.03 eV are major contribution to Na 2p and Mg 2p.

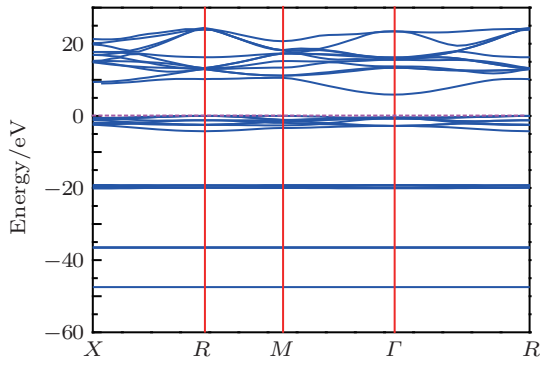


Fig. 2. (color online) The electronic band structure of $NaMgF_3$.

Table 2. The band-gap energies E_g(eV) and the symmetry of the valence-to-conduction band transition for cubic $NaMgF_3$.

	$\Gamma \to X$	$\Gamma \to R$	$\Gamma \to M$	$\Gamma \to \Gamma$	$X \to X$	$R \to R$	$R \to \Gamma$	$M \to M$
E_g	9.39	10.68	11.00	6.36	9.48	10.21	5.90	10.55

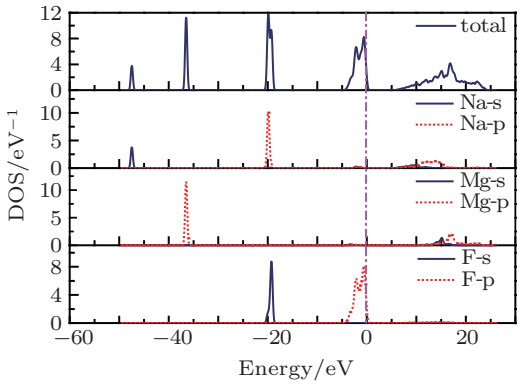


Fig. 3. (color online) The calculated total and partial density of states for cubic $NaMgF_3$.

Mulliken population analysis[36,37] is a good method for studying the bonding behavior and understanding the charge transfer between the cation and anion. Our calculated population analysis results are shown in Table 3. The positive charge values represent the losing electron, and the negative values represent the accepting electron. The charge transfer from Na and Mg to F is about 0.30e and 2.03e, respectively. It can be concluded that the Mg atom has a stronger ability to lose electrons compared to the Na atom. The charge density distributions serve as a complementary tool to understand the electronic structure of the system. The charge density distribution along the (111) plane of cubic $NaMgF_3$ is shown in Fig. 4. The covalent character of any material can be related to the sharing of the charge between the cation and anion, while the ionic character is related to the transfer between the cation and anion. The covalent character of $NaMgF_3$ is due to the hybridization of Na 2p with F 2s states around 21.00 eV. It can be seen that most of the charge is populated in the F–Na bond direction, while the maximum charge resides on the F and Na sites. We also performed Mulliken overlap populations[36,38] of cubic $NaMgF_3$ to describe the interaction between atoms, as listed in Table 4. The positive overlap populations indicate the bonding between the atoms, while the negative represents anti-bonding, and the values denote the intensity of bonding. It is found that a mixture of ionic and weak covalent chemical bonding exists in NaF, and a strong ionic bonding in MgF_2. Hence, cubic $NaMgF_3$ is a mixture bonding material. In particular, our calculated bond length of Mg–F is 1.936 Å, in perfect agreement with the experimental data 1.937 Å at 4 GPa at a temperature of 1000 °C.[18]

Table 3. Mulliken population analysis of $NaMgF_3$.

Species	s	p	Total	Charge/e
F	2.00	5.77	7.78	–0.78
Na	2.30	6.40	8.70	0.30
Mg	0.29	5.68	5.97	2.03

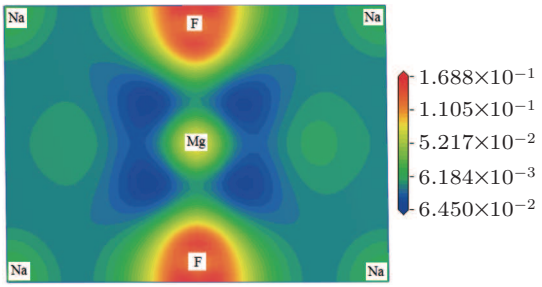


Fig. 4. (color online) Charge density on the (111) plane of cubic $NaMgF_3$.

Table 4. Mulliken overlap populations of $NaMgF_3$.

Bond	Population	Length/Å
F–F	–0.22	2.738
F–Na	0.52	2.738
F-Mg	–3.30	1.936

3.3. Optical properties

The complex dielectric function $\varepsilon(\omega) = \varepsilon_1(\omega) + i\varepsilon_2(\omega)$ is known to describe the optical properties of materials, where ε_1 and ε_2 are the real and imaginary components of the dielectric function, respectively. The excitonic effects are ignored, while the local field effect is included under calculations. The imaginary part $\varepsilon_2(\omega)$ is directly related to the electronic band structure of a material and can describe the absorptive behavior. The interband contribution to the imaginary part of the

dielectric function is calculated by summing all possible transitions from occupied to unoccupied states, and then the imaginary part of the dielectric function $\varepsilon_2(\omega)$ is given by[39–41]

$$\varepsilon_2(\omega) = \left(\frac{4\pi^2 e^2}{m^2\omega^2}\right)\sum_{i,j}\int_k \langle i|M|j\rangle^2 f_i(1-f_i) \times \delta\left(E_{j,k}-E_{i,k}-\omega\right)\mathrm{d}^3k, \quad (1)$$

where e is the charge of free electrons, m is the mass of free electrons, ω is the frequency of incident photons, M is the dipole matrix, i and j are the initial and final states, respectively, f_i is the Fermi distribution function for the i-th state, and E_i the energy of the electron in the i-th state with crystal wave vector k. The real part $\varepsilon_1(\omega)$ of the complex dielectric function can be obtained using the Kramers–Kronig relationship in the form[39–41]

$$\varepsilon_1(\omega) = 1 + \frac{2}{\pi}P\int_0^\infty \frac{\omega'\varepsilon_2(\omega')\,\mathrm{d}\omega'}{\left(\omega'^2-\omega^2\right)}, \quad (2)$$

where P denotes the principal value of the integral. The refractive index $n(\omega)$ and extinction coefficient $k(\omega)$ deduced by the real and imaginary parts of the complex dielectric function can also illuminate the optical properties of substance[39–41]

$$n(\omega) = \left[\frac{\sqrt{\varepsilon_1(\omega)^2+\varepsilon_2(\omega)^2}}{2}+\frac{\varepsilon_1(\omega)}{2}\right]^{1/2}, \quad (3)$$

$$k(\omega) = \left[\frac{\sqrt{\varepsilon_1(\omega)^2+\varepsilon_2(\omega)^2}}{2}-\frac{\varepsilon_1(\omega)}{2}\right]^{1/2}. \quad (4)$$

To give an overview of the optical properties of cubic $NaMgF_3$, we also calculated some other optical constants such as reflectivity $R(\omega)$, absorption coefficient $I(\omega)$, electron energy loss spectrum $L(\omega)$, and optical conductivity $\sigma(\omega)$. The relationships are as follows:[39–41]

$$R(\omega) = \left|\frac{\sqrt{\varepsilon(\omega)}-1}{\sqrt{\varepsilon(\omega)}+1}\right|^2, \quad (5)$$

$$I(\omega) = \sqrt{2}(\omega)\left[\sqrt{\varepsilon_1(\omega)^2+\varepsilon_2(\omega)^2}-\varepsilon_1(\omega)\right]^{1/2}, \quad (6)$$

$$L(\omega) = \frac{\varepsilon_2(\omega)}{\varepsilon_1(\omega)^2+\varepsilon_2(\omega)^2}, \quad (7)$$

$$\sigma(\omega) = \sigma_1(\omega)+\mathrm{i}\sigma_2(\omega) = -\mathrm{i}\frac{\omega}{4\pi}[\varepsilon(\omega)-1]. \quad (8)$$

The real and imaginary parts of the dielectric function are displayed in Fig. 5. From the real dielectric function $\varepsilon_1(\omega)$, information about the electronic polarizability of the material can be obtained. The static dielectric constant within the zero frequency limit is obtained as $\varepsilon_1(0) = 1.95$. There are two negative scales for the ranges 54.14–54.62 eV and 58.53–61.00 eV. This indicates that the cubic perovskite $NaMgF_3$ shows a metallic behavior in these frequency zones. In the curve $\varepsilon_2(\omega)$, there are mainly nine peaks, which are identified by the symbols A (0.75 at 9.70 eV), B (1.17 at 12.19 eV), C (0.97 at 14.29 eV), D (2.08 at 17.39 eV), E (0.11 at 36.36 eV), F (1.95 at 51.74 eV), G (2.56 at 53.30 eV), H (1.04 at 55.95 eV), and I (1.32 at 58.24 eV). Peak A is mainly due to the transition from F 2p (at −0.95 eV) in the valence band to Na 3s (at 8.93 eV) in the conduction band at the X-point. Peak B may be due to the electronic transitions from F 2p (at −1.14 eV) to Na 2p (at 11.16 eV) at the M-point. Peak C arises from the transitions: F 2p (at −0.71 eV) to Na 2p (13.34 eV) at the Γ-point and F 2p (at −4.25 eV) to Na 3s (10.21 eV) at the R-point. Peak D originates from the following transitions: F 2p (at −0.01 eV) to Mg 2p (at 17.31 eV) at M-point, F 2p (at −2.41 eV) to Na 2p and Mg 3s (at 14.91 eV) at the X-point, F 2p (at −1.24 eV) to Mg 2p (at 16.26 eV) and F 2p (at −4.25 eV) to Na 2p (at 13.20 eV) at the R-point, respectively. Peak E is a significant contribution from F 2s (at −19.24 eV) to Mg 2p (17.28 eV) at the M-point and Na 2p (at −20.10 eV) to Mg 2p (16.14 eV) at the Γ-point. Peak F emerges from Mg 2p (at −36.49 eV) to Mg 3s (15.26 eV) at the X-point, and Mg 2p (at −36.50 eV) to Mg 3s (15.21 eV) at the M-point. Peak G arises from the transitions Mg 3s (at −36.49 eV) to Mg 2p (at 16.91 eV) at the X-point, and peak H originates from Mg 3s (at −36.49 eV) to Mg 2p (19.77 eV) at the X-point. Peak I is mainly due to the transition from Na 3s (at −47.45 eV) to Na 2p (at 11.16 eV) at the M-point. The threshold energy of the dielectric function occurs at $E_0 = 5.90$ eV, which corresponds to the fundamental gap at equilibrium. It is well known that materials with band gaps larger than 3.1 eV work well in the ultraviolet region of the spectrum.[42,43] Therefore, $NaMgF_3$ will work excellently in the UV region as an optical material.

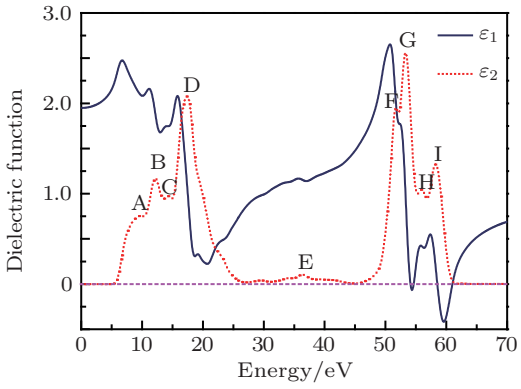


Fig. 5. (color online) The calculated $\varepsilon_1(\omega)$ real and $\varepsilon_2(\omega)$ imaginary parts of the complex dielectric constant of cubic $NaMgF_3$.

The calculated refractive index $n(\omega)$ and extinction coefficient $k(\omega)$ are depicted in Fig. 6. The static refractive index $n(0)$, which implies the important quantity, has the value 1.40, which is similar to the experimental result for the orthorhombic structure for $NaMgF_3$ ($n = 1.364$).[19] The maximum refractive index is 1.67 at 51.00 eV. In the $k(\omega)$ curve, the local

maximum of the extinction coefficient $k(\omega)$ corresponds to the zero of $\varepsilon_1(\omega)$ (≈ 53.81 eV).

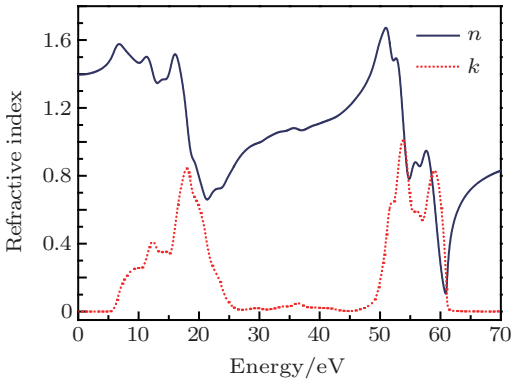


Fig. 6. (color online) The calculated refractive index $n(\omega)$ and the extinction coefficient $k(\omega)$ of cubic $NaMgF_3$.

The optical absorption coefficient $I(\omega)$ of cubic $NaMgF_3$ is shown in Fig. 7. The absorption edge E_{op} can be obtained from the following relation:[44]

$$\alpha h\nu = C\left(h\nu - E_{op}\right)^n, \tag{9}$$

where $h\nu$ is the photon energy, C is a constant, and α is the optical absorption coefficient. We use $n = 0.5$ for a direct band-gap material and $n = 2$ for an indirect band-gap material. Using the linear extrapolation method, the indirect absorption edge with phonon absorption ($E_g^{indir} - E_{ph}$) is determined to be 5.49 eV, where E_g^{indir} is the indirect band gap and E_{ph} the phonon energy. This shows that the absorption edge starts from about 5.49 eV, after which the intensity varies with the increase in photon energy, and reaches a maximum value of 8.74×10^5 at 53.81 eV. There is no electronic transition in the low energy range ($E < 5.49$ eV) because the energy of the photon is lower than the band gap of the material. The first peak in the absorption spectrum occurs at 12.48 eV, and other peaks occur at 18.09 eV, 36.39 eV, 53.81 eV, 56.10 eV, and 59.05 eV, respectively.

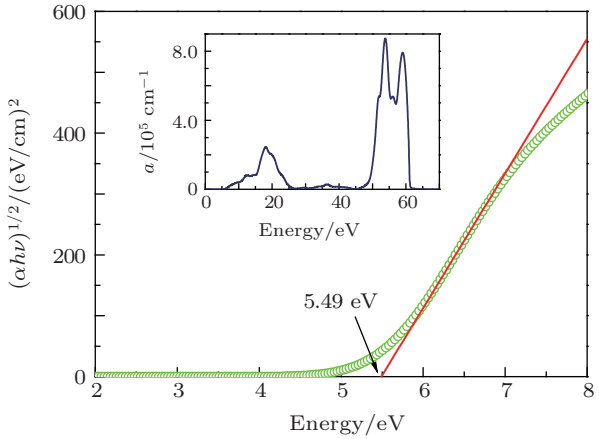


Fig. 7. (color online) The calculated optical absorption coefficient and variation of $(\alpha E)^{1/2}$ as a function of photon energy for cubic $NaMgF_3$.

The calculated electron energy loss spectrum $L(\omega)$, reflectivity $R(\omega)$, and optical conductivity $\sigma(\omega)$ of cubic $NaMgF_3$ are shown in Fig. 8. The loss function is an important parameter describing the energy loss of a fast electron traversing in a material. Generally, the peak of the $L(\omega)$ spectrum represents the characteristic associated with the plasma resonance, and the corresponding frequency is the so-called plasma frequency ω_p. Figure 8(a) shows that the resonant energy loss occurs at 61.00 eV. The reflectivity $R(\omega)$ is displayed in Fig. 8(b). The zero-frequency reflectivity is 2.73%, which remains almost the same up to about 5.50 eV. The small value of reflectivity, as well as the absorption coefficient in the infrared and visible energy range, predicts that the material is transparent in this range. Interestingly, the synthetic neighborite with a composition of $NaMgF_3$ and perovskite structure was confirmed to be colorless and transparent,[19] and thus can be used as an anti-reflection coating material in this region of 0–5.5 eV. Moreover, it may be more practical compared with some of the other metal fluorides because of its lower reflectivity.[9,45,46] The maximum reflectivity value is 67.07%, which occurs at 60.86 eV. Remarkably, the maximum energy loss function occurs while the real part of the dielectric function $\varepsilon_1(\omega)$ goes below zero and the reflectivity starts decreasing rapidly, as can be seen in Figs. 6, 8, and 9. Finally, the optical conductivity $\sigma(\omega)$ of cubic $NaMgF_3$ is also depicted in Fig. 8.

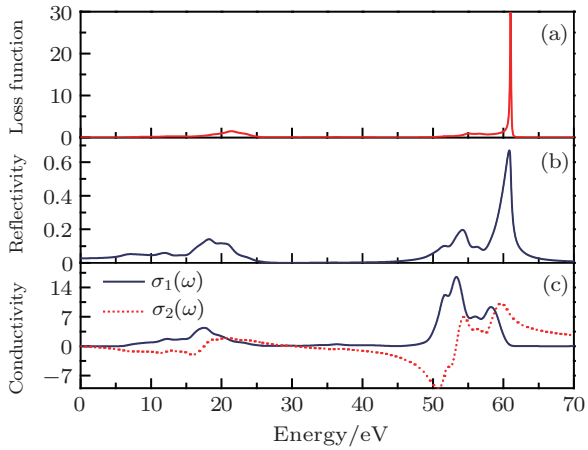


Fig. 8. (color online) Optical spectra as a function of photon energy for cubic $NaMgF_3$: (a) energy loss function, (b) reflectivity, and (c) optical conductivity.

4. Conclusion

In summary, the structural, electronic, and optical properties of cubic perovskite $NaMgF_3$ were calculated by performing density functional theory with local density approximations. The lattice constant a_0, equilibrium volume V_0, bulk modulus B_0 , and its derivative of bulk modulus B_0' were obtained by fitting to the Birch–Murnaghan equation of state. The electronic band structure shows that cubic $NaMgF_3$ has a wide indirect band gap of 5.90 eV. Cubic $NaMgF_3$ has strong

ionic bonding in MgF_2 and a mixture of ionic and weak covalent bonding in NaF. We also investigated the dielectric function, refractive index, absorption coefficient, energy loss spectroscopy, reflectivity, and optical conductivity in detail. The static dielectric constant is obtained as $\varepsilon(0) = 1.95$. Cubic perovskite $NaMgF_3$ shows dielectric behavior. Using the linear extrapolation method, the absorption edge E_g is determined to be 5.49 eV. Besides, the material shows high transmittance and low reflectivity in the 0–5.5 eV region. Thus, it can be used as an anti-reflection coating material.

References

[1] El Ouenzerfi R, Ono S, Quema A, Goto M, Sakai M, Sarukura N, Nishimatsu T, Terakubo N, Mizuseki H, Kawazoe Y, Sato H, Ehrentraut D, Yoshikawa A and Fukuda T 2004 *J. Appl. Phys.* **96** 7655

[2] Shimamura K, Sato H, Bensalah A, Sudesh V, Machida H, Sarukura N and Fukuda T 2001 *Cryst. Res. Technol.* **36** 801

[3] Setter N, Damjanovic D, Eng L, Fox G, Gevorgian S, Hong S, Kingon A, Kohlstedt H, Park N Y, Stephenson G B, Stolitchnov I, Taganstev A K, Taylor D V, Yamada T and Streiffer S 2006 *J. Appl. Phys.* **100** 051606

[4] Lim S H, Rastogi A C and Desu S B 2004 *J. Appl. Phys.* **96** 5673

[5] Cooke A H, Jones D A, Silva J F A and Wells M R 1975 *Solid State Phys.* **8** 4083

[6] Springis M, Sharakovsky A, Tale I and Rogulis U 2005 *Phys. Status Solidi C* **2** 511

[7] Nishimatsu T, Terakubo N, Mizuseki H, Kawazoe Y, Pawlak D A, Shimamura K and Fukuda T 2002 *Jpn. J. Appl. Phys.* **41** 365

[8] Knierim W, Honold A, Brauch U and Durr U 1986 *J. Opt. Soc. Am. B* **3** 119

[9] Babu K E, Veeraiah A, Swamy D T and Veeraiah V 2012 *Chin. Phys. Lett.* **29** 117102

[10] Hörsch G and Paus H J 1986 *Opt. Commun.* **60** 69

[11] Fukuda T, Shimamura K, Yoshikawa A and Villora E G 2001 *Optoelectron. Rev.* **9** 109

[12] Takahashi H and Onaka R 1977 *J. Phys. Soc. Jpn.* **43** 2021

[13] Chao E C T, Evans H T, Skinner B J and Milton C 1961 *Am. Mineral.* **46** 379

[14] Zhao Y, Weidner D J, Parise J B and Cox D E 1993 *Phys. Earth Planet. Inter.* **76** 1

[15] Zhao Y, Weidner D J, Parise J B and Cox D E 1993 *Phys. Earth Planet. Inter.* **76** 17

[16] Zhao Y, Weidner D J, Ko J, Leinenweber K, Liu X, Li B, Meng Y, Pacalo R E G, Vaughan M T, Wang Y and Yeganeh-Haeri A 1994 *J. Geophys. Res.* **99** 2871

[17] Zhao Y, Parise J B, Wang Y B, Kusaba K, Vaughan M T, Weidner D J, Kikegawa T, Chen J H and Shimomura O 1994 *Am. Mineral.* **79** 615

[18] Chen J, Liu H, Martin C D, Parise J B and Weidner D J 2005 *Am. Mineral.* **90** 1534

[19] Zhao Y and Weidner D J 1993 *Phys. Chem. Miner.* **20** 419

[20] Andersen N H, Kjems J K and Hayes W 1985 *Solid State Lonics* **17** 143

[21] Seretlo J R, Martin J J and Sonder E 1976 *Phys. Rev. B* **14** 5404

[22] Sevonkaev I, Goia D V and Matijević E 2008 *J. Colloid Interface Sci.* **317** 130

[23] Zhang X M, Quan Z W, Yang J, Yang P P, Lian H Z and Lin J 2009 *J. Colloid Interface Sci.* **329** 103

[24] Li L and Weidner D J 2012 *Phys. Earth Planet. Inter.* **194–195** 98

[25] Hohenberg P and Kohn W 1964 *Phys. Rev. B* **136** 864

[26] Vanderbilt D 1990 *Phys. Rev. B* **41** 7892

[27] Ceperley D M and Alder B J 1980 *Phys. Rev. Lett.* **45** 566

[28] Perdew J P and Wang Y 1992 *Phys. Rev. B* **45** 13244

[29] Pack J D and Monkhorst H J 1977 *Phys. Rev. B* **16** 1748

[30] Segall M D, Lindan P J D, Probert M J, Pickard C J, Hasnip P J, Clark S J and Payne M C 2002 *J. Phys.: Condens. Matter* **14** 2717

[31] Milman V, Winkler B, White J A, Packard C J, Payne M C, Akhmatskaya E V and Nobes R H 2000 *Int. J. Quantum Chem.* **77** 895

[32] Murnaghan F D 1944 *Proc. Natl. Acad. Sci. USA* **30** 244

[33] Martin C D, Chupas P J, Chapman K W and Parise J B 2007 *J. Appl. Crystallogr.* **40** 441

[34] Luaña V, Costales A and Pendás A M 1997 *Phys. Rev. B* **55** 4285

[35] Geguzina G A and Sakhnenko V P 2004 *Crystall. Rep.* **49** 15

[36] Mulliken R S 1955 *J. Chem. Phys.* **23** 1833

[37] Segall M D, Pickard C J, Shah R and Payne M C 1996 *Mol. Phys.* **89** 571

[38] Segall M D, Shah R, Pickard C J and Payne M C 1996 *Phys. Rev. B* **54** 16317

[39] Ambrosch D C and Sofo J O 2006 *Comput. Phys. Commun.* **175** 1

[40] Fox M 2001 *Optical Properties of Solids* (New York: Oxford University Press)

[41] Wooten F 1972 *Optical Properties of Solids* (New York: Acadmic Press) p. 179

[42] Maqbool M, Amin B and Ahmed I 2009 *J. Opt. Soc. Am. B* **26** 2181

[43] Maqbool M, Kordesch M E and Kayani A 2009 *J. Opt. Soc. Am. B* **26** 998

[44] Srikant V and Clarke D R 1997 *J. Appl. Phys.* **81** 6357

[45] Murtaza G, Ahmad I, Maqbool M, Rahnamaye Aliabad H A and Afaq A 2011 *Chin. Phys. Lett.* **28** 117803

[46] Secuk M N, Dogan E K, Aycibin M, Erdinc B and Akkus H 2013 *Am. J. Mod. Phys.* **2** 77